Available online at www.sciencedirect.com

SciVerse ScienceDirect

Ceramics International 38 (2012) 2963–2970

CERAMICS INTERNATIONAL

www.elsevier.com/locate/ceramint

Frequency and temperature dependent electrical properties of $Ni_{0.7}Zn_{0.3}Cr_xFe_{2-x}O_4$ ($0 \leq x \leq 0.5$)

A.A. Birajdar [a], Sagar E. Shirsath [b,*], R.H. Kadam [c], S.M. Patange [c], D.R. Mane [d], A.R. Shitre [e]

[a] Department of Physics, SMP College, Murum, Osmanabad (MS), India
[b] Department of Physics, Vivekanand College, Aurangabad 431004 (MS), India
[c] Materials Research Laboratory, Srikrishna Mahavidyalaya Gunjoti, Omerga, Osmanabad 413613 (MS), India
[d] Department of Physics, Balbhim College, Beed (MS), India
[e] Department of Physics, YC College, Tuljapur, Osmanabad (MS), India

Received 3 May 2011; received in revised form 23 November 2011; accepted 28 November 2011
Available online 7 December 2011

Abstract

Series of the ferrite samples with a chemical formula $Ni_{0.7}Zn_{0.3}Cr_xFe_{2-x}O_4$ ($x = 0.0$–0.5) were prepared by a sol–gel auto-combustion method and annealed at 600 °C for 4 h. The prepared samples have the cubic spinel structure with no impurity phase. As the Cr^{3+} content x increases, the unit cell dimensions decrease with an increase in Cr^{3+} content x. The crystallite size is decreases from 37 nm to 21 nm as the Cr^{3+} content increases from $x = 0.0$ to 0.5. Resistivity increases whereas dielectric constant decreases with an increase in Cr^{3+} content x. Maxima in the dielectric loss tangent versus frequency appear when the frequency of the hopping charge carriers coincides with the frequency of the applied alternating field. Dielectric constant and dielectric loss tangent increases with increase in temperature. Saturation magnetization of sintered samples showed higher values as compared to as-prepared sample. Curie temperature deduced from AC susceptibility data decreases with increasing x.

PACS : 75.50.Gg; 77.22.−d; 72.15.Cz

Keywords: C. Dielectric properties; Nanocrystalline ferrites; Conduction mechanism; D.C. resistivity

1. Introduction

Ni–Zn ferrites are one of the most versatile soft magnetic materials. Recently, the technological application of these materials has been studied extensively, primarily due to their applicability in many electronic devices owing to their, high permeability at high frequency, remarkably high-electrical resistivity, low-eddy current loss and reasonable cost [1,2]. Ferrites with good dielectric properties have a large number of applications from microwave to radio frequencies. High electrical resistivity and low magnetic coercivity make Ni–Zn ferrite a technologically important material for applications in the mega-hertz frequency region. The performance characteristics of Ni–Zn ferrites in this frequency region are being improved by following a variety of synthetic approaches and selective grain and grain-boundary doping [3].

The spinel structure of these ferrites possesses the general formula of $(A)[B_2]O_4$, where A represents cations in tetrahedral sites and B represents cations in the octahedral positions in a cubic structure. However, the formula $(A_{1-i}B_i)[AiB_{2-I}]O_4$ represents many possible intermediary distributions that denote considerable cation disorder, indicating that this structure requires special attention in terms of structural and electrical properties. The Ni–Zn ferrite is a well-known mixed inverse spinel, whose unitary cell is represented by the formula $(Zn_xFe_{1-x})[Ni_{1-x}Fe_{1+x}]O_4$ [4]. The addition of impurities induces changes in the defect structure and texture of the crystal [5], creating significant modifications in the magnetic and electrical properties of these materials. Chromium (Cr^{3+}) ions with antiferromagnetic nature are known for achieving control over magnetic parameters in developing technologically important materials. Chromium could produce sufficient changes in $(A)[B_2]O_4$

* Corresponding author. Tel.: +91 02402240950; fax: +91 02402361270.
E-mail address: shirsathsagar@hotmail.com (S.E. Shirsath).

0272-8842/$36.00
doi:10.1016/j.ceramint.2011.11.074

solution and known that Cr^{3+} ions have strong B-site preference. Cr^{3+} has a weaker magnetic moment than Fe, the partial replacement of Fe by Cr ion cause magnetic frustration [6]. Several researchers have studied the effects of Cr-substitution in the spinel structure of ferrites [5,7,8]. However, we have not found any report related to electrical properties in the literature on Cr^{3+} substituted Ni–Zn ferrite powders obtained by sol–gel auto-combustion reaction. It could also be interesting to study the importance of electrical properties of Ni–Zn ferrite and also the possible influence of addition of Cr^{3+} on the electric conduction of Ni–Zn ferrite. This paper therefore presents a study of electrical properties of nano-size Ni–Zn ferrite doped with Cr^{3+} synthesized by sol–gel auto-combustion synthesis.

2. Materials and methods

The powders were synthesized by the sol–gel auto-combustion method [9,10]. A.R. grade citric acid ($C_6H_8O_7{\cdot}H_2O$), nickel nitrate ($Ni(NO_3)_2{\cdot}6H_2O$), zinc nitrate ($Zn(NO_3)_2{\cdot}6H_2O$), chromium nitrate ($Cr(NO_3)_3{\cdot}9H_2O$) and iron nitrate ($Fe(NO_3)_3{\cdot}9H_2O$) were dissolved in distilled water to obtain a mixed solution. The reaction procedure was carried out in an air atmosphere without the protection of inert gases. The molar ratio of metal nitrates to citric acid was 1:3. The metal nitrates were dissolved together in the minimum amount of double-distilled water needed to obtain a clear solution. An aqueous solution of citric acid was mixed with the metal-nitrate solution, and ammonia solution was slowly added to adjust the pH to 7. The mixed solution was placed on a hot plate with continuous stirring at 90 °C. During evaporation, the solution formed a very viscous brown gel. When all of the water molecules were removed from the mixture, the viscous gel began to froth. After a few minutes, the gel ignited and burnt with glowing flints. The decomposition reaction continued until the entire citrate complex was consumed. The auto-combustion was completed within a minute, yielding brown-colored ashes referred to here as the precursor. The prepared powders of all the samples were annealed at 600 °C for 4 h to obtain the final product. The detail procedure of the sol–gel combustion technique is reported in our previous publications.

The samples were X-ray examined by Phillips X-ray diffractometer (Model 3710) with Cu-K_α radiation ($\lambda = 1.5405$ Å). Morphology and structure of the powder samples were studied on JEOL-JSM-5600 N scanning electron micrograph (SEM). The D.C. electrical resistivity of each sample was measured using the two-probe technique in the temperature range of 300–800 K on a disc shaped pellet of 10 mm diameter and 3 mm thickness using two probe technique. The dielectric properties such as dielectric constant (ε') and dielectric loss tangent ($\tan\delta$) were studied using LCR-Q meter (Hioki) at room temperature and in the frequency range of 100 Hz to 1 MHz. The dielectric constant (ε') and the dielectric-loss tangent ($\tan\delta$) are also carried out as a function of temperature in the temperature ranges from 403 to 773 K.

3. Results and discussion

The X-ray diffraction (XRD) patterns of the $Ni_{0.7}Zn_{0.3}Cr_xFe_{2-x}O_4$ spinel ferrite system sintered at 600 °C for 4 h are shown in Fig. 1. All of the Bragg peaks of the XRD patterns are broad and do not contain any extra peak other than cubic spinel phase. The lattice constant 'a' of all the samples was determined by using the equation discussed elsewhere [10]. It is found that the lattice constant decreases from 8.363 to 8.333 Å with increase in Cr^{3+} content x. The decrease in the lattice constant is related to the difference in ionic radii of Fe^{3+} and Cr^{3+}. In the present ferrite system, Fe^{3+} ions (0.67 Å) ions are replaced by the relatively small Cr^{3+} ions (0.64 Å). The average crystallite size (t) was determined using the line broadening of the main reflection (3 1 1) and (4 4 0) diffraction peak using the Debye Scherrer formula [11]. The crystallite size is decreases from 37 nm to 21 nm with increasing Cr^{3+} content.

The SEM micrographs for the as prepared (combustion powder) and sintered samples are shown in Fig. 2 (a) and (b) respectively. It is evident from these figures that the microstructure of these samples is affected by Cr^{3+} substitution. The sintered density 'd_B' of the specimens was determined by Archimedes' method and using following equation.

$$d_B = \left[\frac{W_a}{W_a - W_W}\right] \text{g/cc} \quad (1)$$

where W_a is the weight of the sample in air, W_w is the weight of sample in water. The density of water is taken as 0.995 g/cm^3 (at 30 °C). The variation of sintered density is shown in Fig. 3. The sintered density was found to decrease with increasing Cr content x. In the present series, both the molecular weight of the $Ni_{0.5}Zn_{0.5}Fe_2O_4$ spinel ferrite and the volume of the unit cell decrease with increasing Cr substitution, but the rate of the

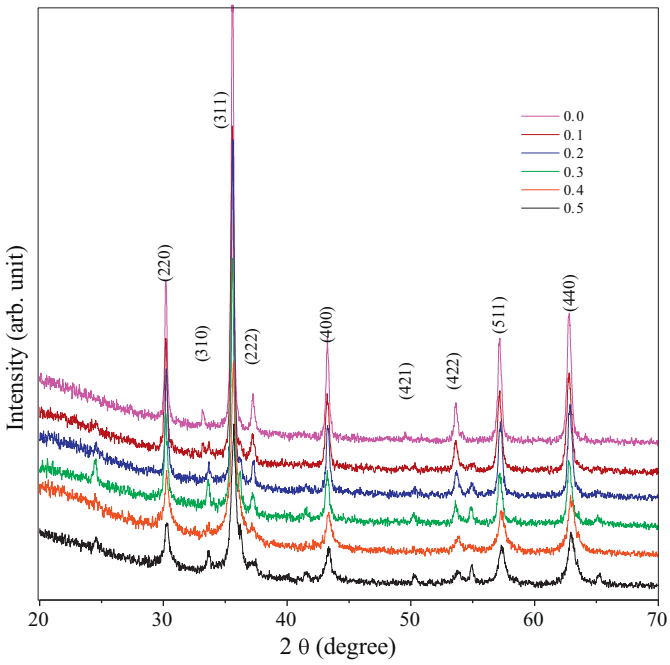

Fig. 1. X-Ray diffraction patterns of $Ni_{0.7}Zn_{0.3}Cr_xFe_{2-x}O_4$.

decrease of molecular weight is more than that of volume. Therefore, the sintered density decreases with Cr substitution in the present case. This led to increase in porosity. The porosity '*P*' of the ferrite nano particles was then determined using the following relation,

$$P = 1 - \frac{d_B}{d_x} \quad (2)$$

where d_B and d_x are the sintered and X-ray densities respectively. The variation of porosity with Cr content x is shown in Fig. 3. It is clear from Fig. 3 that the sample density decreases and the porosity increases with increasing Cr content. The increase in porosity may be due to the decrease in particle size, which increases the grain boundaries of the particle and accordingly the porosity. The high porosity demonstrates the porous structure of the prepared Ni–Zn–Cr–Fe spinel ferrite samples.

3.1. D.C. resistivity

Fig. 4 shows the variation of D.C. resistivity with the Cr^{3+} concentration for all of the investigated samples. The D.C. resistivity shows a linear decrease with temperature. This variation is explained by the location of the cations in the spinel ferrite. It is seen that the variation in D.C. resistivity is almost linear up to a certain temperature, at which a break occurs. This break corresponds to the Curie temperature, indicating a change of magnetic ordering from ferrimagnetism to paramagnetism. An increase in resistivity is observed with an increase in Cr^{3+} concentration (Fig. 5). In ferrites, the resistivity (ρ) at an

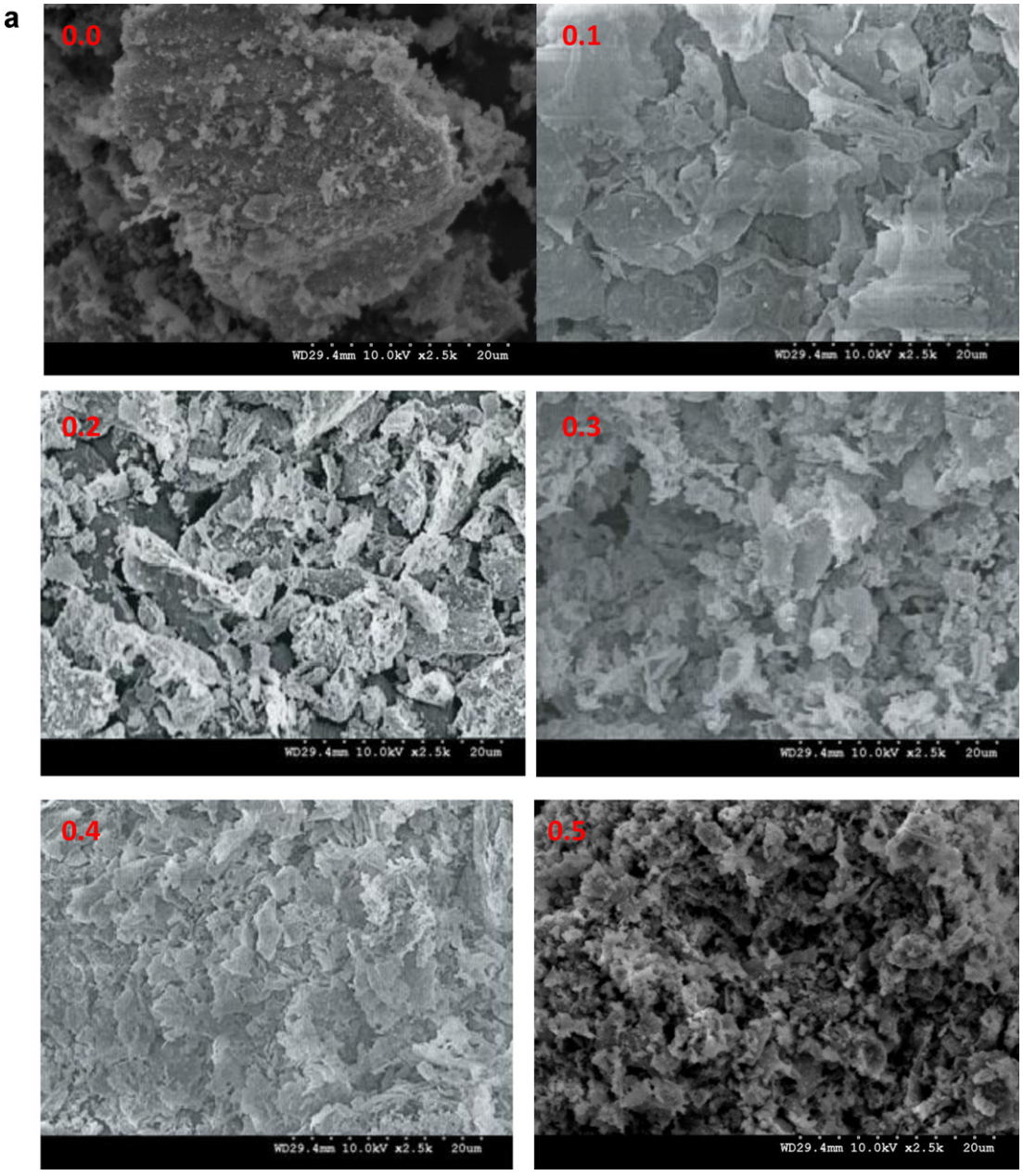

Fig. 2. (a) SEM images for the as prepared samples. (b) SEM images for the samples sintered at 600 °C.

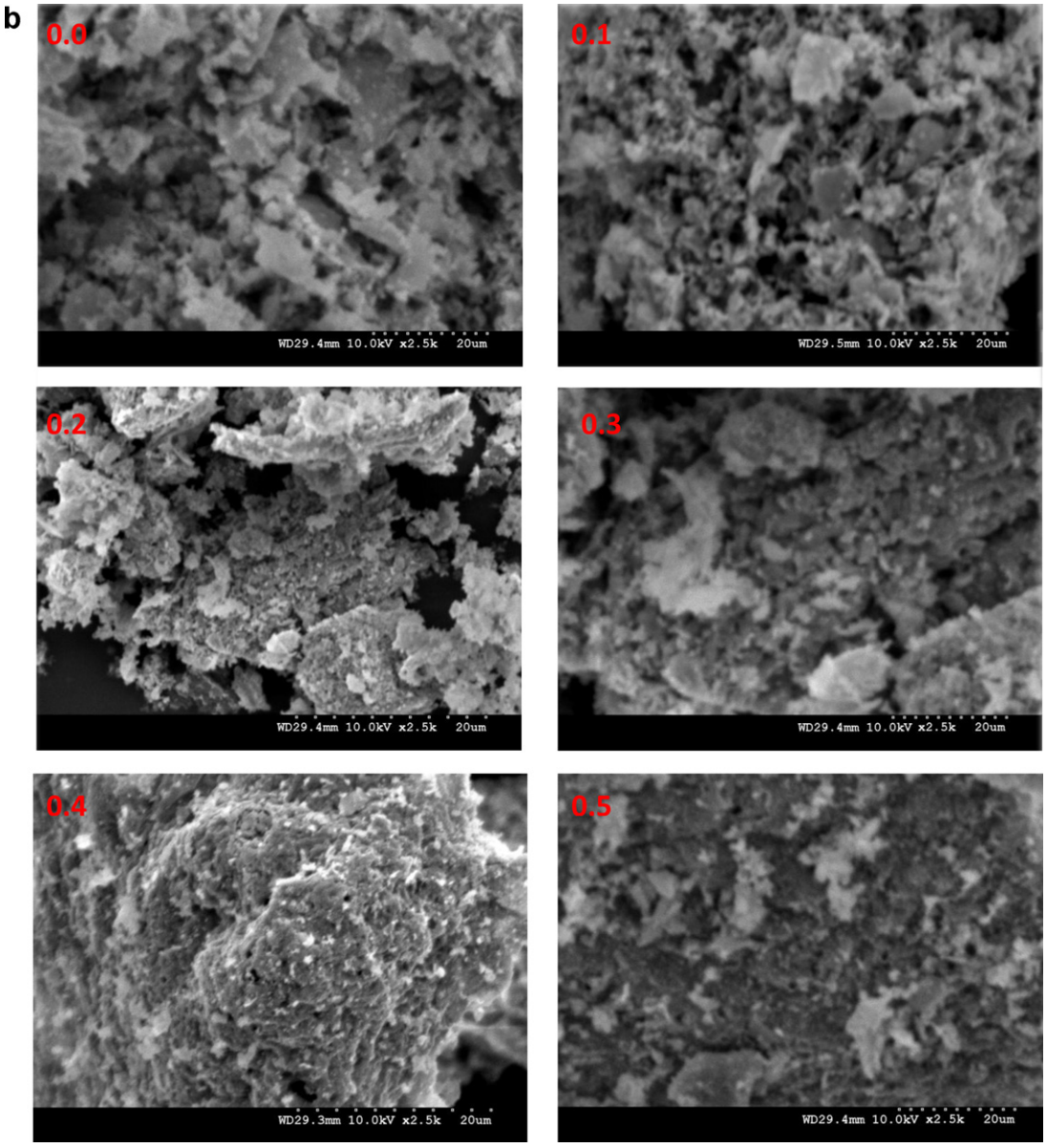

Fig. 2. (*Continued*).

absolute temperature T is given by the Arrhenius relation, $\rho = \rho_0 e^{-\mathrm{Eg}/kT}$, where Eg is the activation energy and k is Boltzmann constant. The values of activation energy are listed in Table 1. In the table, E_f is the activation energy corresponding to the ferrimagnetic region and E_p is that corresponding to the paramagnetic region. It is apparent that the activation energies in the paramagnetic region are higher than those in the ferrimagnetic region. This finding can be attributed to the disordered states of the paramagnetic region and the ordered states of the ferrimagnetic region. This result also suggests that the conduction process is affected by the change in magnetic ordering. The electrical conduction in ferrites can be explained by the Verwey model of electron hopping which involves the exchange of electron between ions of the same element present in different valance states, and distributed randomly over crystallographically equivalent lattice sites. In the present system, the conduction is attributed to the exchange of 3d electron between Fe^{2+} and Fe^{3+} ions in the octahedral B-site. A small amount of Fe^{3+} is converted in to Fe^{2+} during sintering. The observed increase in resistivity can be understood by considering the hopping mechanism, $Fe^{2+} \leftrightarrow Fe^{3+}$.

Table 1
Activation energy of ferrimagnetic (E_f), paramagnetic (E_p) region and resultant activation energy (ΔE) of $Ni_{0.7}Zn_{0.3}Fe_{2-x}Cr_xO_4$.

Comp. x	E_p (eV)	E_f (eV)	ΔE (eV)
0.0	0.21	0.11	0.10
0.1	0.26	0.14	0.12
0.2	0.32	0.16	0.16
0.3	0.37	0.19	0.18
0.4	0.43	0.21	0.22
0.5	0.51	0.24	0.27

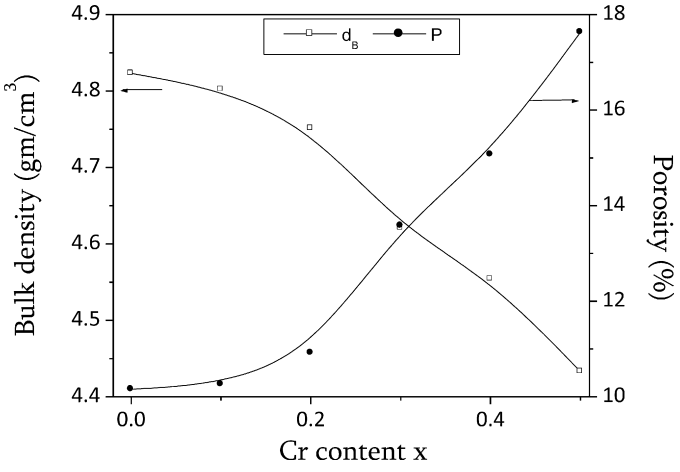

Fig. 3. Variation of sintered density (d_B), and porosity (P) with Cr content x.

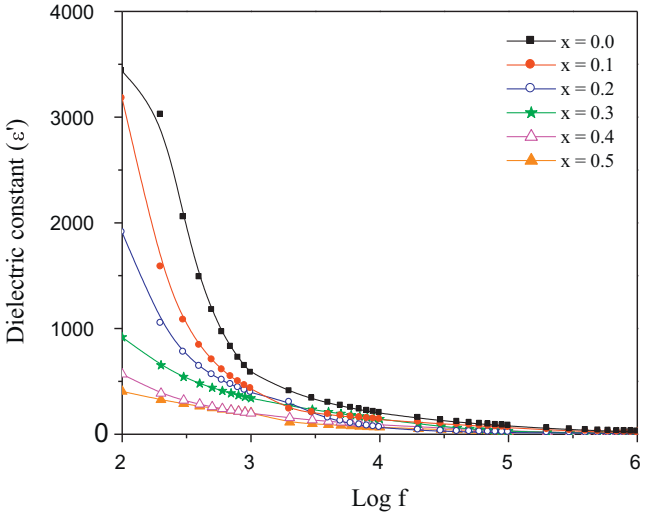

Fig. 6. Variation of dielectric constant with logarithm of frequency.

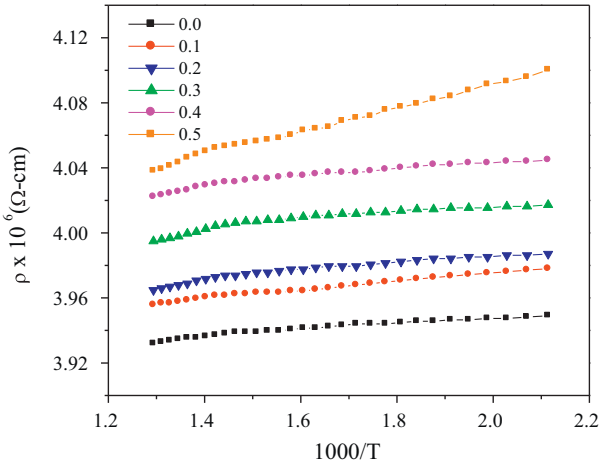

Fig. 4. Variation of resistivity with temperature.

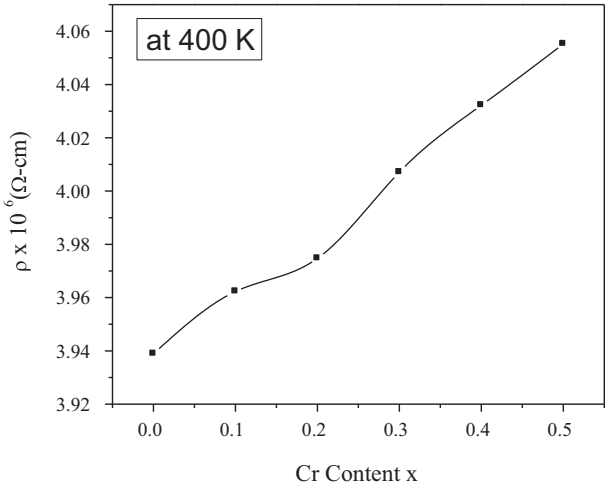

Fig. 5. Variation of resistivity with Cr content x.

The increase in Cr^{3+} ions at B-site leads to replacement of Fe^{3+} ions at B site leads to decrease of ferrous ions formed. Though the Cr^{3+} ions do not participate in conduction mechanism but limit the degree of $Fe^{2+} \leftrightarrow Fe^{3+}$ transfer, thereby obstructing electron hopping [12] resulted in increase in resistivity.

3.2. Frequency dependence of dielectric properties

Fig. 6 shows the variation of the dielectric constant (ε') as a function of frequency. The frequency dependence of dielectric constant for $Ni_{0.7}Zn_{0.3}Cr_xFe_{2-x}O_4$ is in very good agreement with the other spinel ferrite [13] for which the dielectric constant decreases continuously with increasing frequency. It can be seen that the dielectric constant decreases with increasing frequency in the lower frequency region. As frequency increases, the dielectric constant remains almost constant. All of samples displayed dispersion due to Maxwell–Wagner interfacial polarization [14,15] in agreement with Koop's phenomenological theory [16]. The dielectric behavior may be explained qualitatively by supposing that the mechanism of the polarization process in ferrite which is similar to that of the conduction process. Based on the electronic exchange $Fe^{3+} \leftrightarrow Fe^{2+} + e^-$ one obtains the local displacement of the electron in the direction of the applied electric field. It is well-known that the effect of the polarization is to reduce the field inside the medium. The decrease in the polarization of the dielectric constant with increasing frequency is due to fact that at a certain electrical-field frequency, the electron exchange between ferrous and ferric ions cannot keep pace with the alternating field. Therefore, the dielectric constant of the material may decreases substantially as the frequency increases. The variation of the dielectric loss tangent ($\tan\delta$) with the logarithm of frequency ($\log f$) for all compositions is shown in Fig. 7. All of the compositions show normal dielectric behavior and an exponential decrease in the dielectric loss tangent with increasing frequency. A maximum in the dielectric loss tangent versus frequency

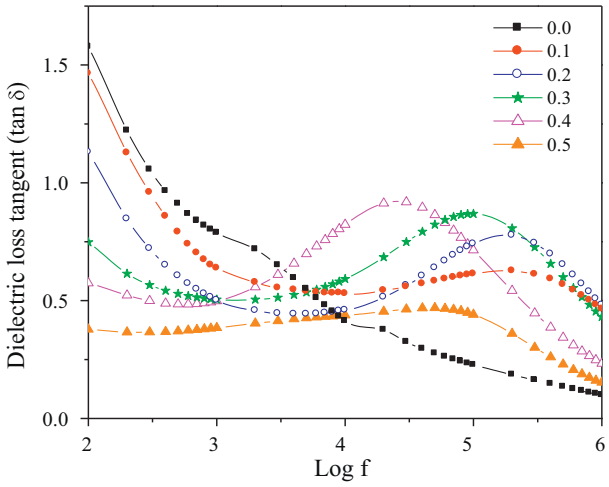

Fig. 7. Variation of dielectric loss tangent with logarithm of frequency.

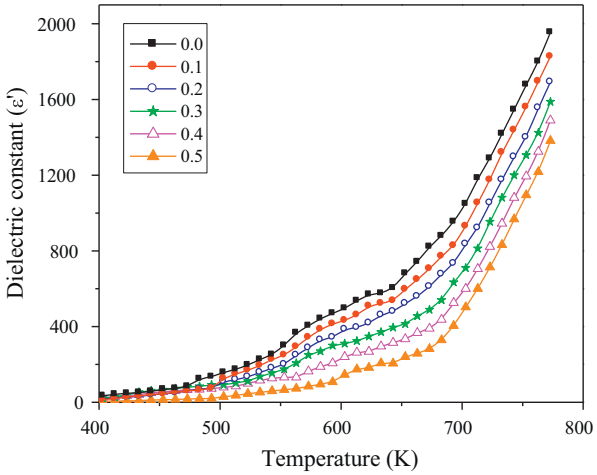

Fig. 8. Variation of dielectric constant with temperature.

appears the when frequency of the hopping charge carriers coincides with the frequency of the applied alternating field. The maxima in the dielectric loss tangent occur at relatively low frequencies and decreases with increasing frequency. The broad peak disappears at higher frequencies. A broad peak of the dielectric loss tangent indicates the existence of a distribution of relaxation time rather than a single relaxation time [17]. The condition for observing maxima in dielectric loss tangent of a material is $\omega\tau = 1$ where $\omega = 2\pi f_{max}$ and τ is the relaxation time. The relaxation time is related to the jumping probability per unit time P by the relation $\tau = (1/2)P$ or $f_{max}\alpha P$.

It is observed that dielectric constant (ε') and dielectric loss tangent (tan δ) deceases with increase in Cr^{3+} content. When Cr^{3+} is added in place of Fe^{3+}, this decreases the hopping between Fe^{2+} and Fe^{3+} ions, thereby increasing the resistance of the grain. This decreases the probability of electrons reaching the grain boundary. As a result, the polarization and, hence, the dielectric constant decrease with increasing Cr^{3+}.

3.3. Temperature dependence of dielectric properties

The dielectric constant (ε'), and the dielectric-loss tangent (tan δ) of $Ni_{0.7}Zn_{0.3}Fe_{2-x}Cr_xO_4$ were computed according to Smit and Wijn [18] as a function of temperature. The measurements were carried out from 403 to 773 K, and Fig. 8 shows the variation of the dielectric constant with temperature at a fixed frequency of 1 kHz. It is clear from the figure that the dielectric constant increases with increasing temperature for all samples. This temperature dependence of the dielectric constant for $Ni_{0.7}Zn_{0.3}Fe_{2-x}Cr_xO_4$ is in very good agreement with spinel ferrite [19,20], for which the dielectric constant increases with increasing temperature.

The variation of the dielectric-loss tangent with temperature is given in Fig. 9, in which it is observed that the dielectric-loss tangent increases with increasing temperature. The increase in the dielectric-loss tangent is fast up to 700 K, but the dielectric-loss tangent decreases beyond this temperature. According to Rabkin and Novikova [21], the process of dielectric polarization

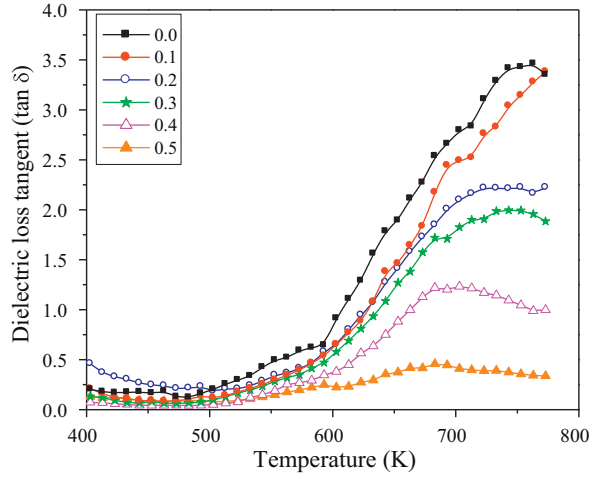

Fig. 9. Variation of dielectric loss tangent with temperature.

in ferrite occurs through a mechanism similar to the conduction process. From the electronic exchange $Fe^{3+} \leftrightarrow Fe^{2+}$ and $Ni^{2+} \leftrightarrow Ni^{3+}$, one obtains the local displacement of the electron in the direction of the applied electrical field. This displacement determines the polarization of both types of charge carrier, n and p, which contributes to the polarization and depends on temperature. The temperature dependence of the dielectric constant and dielectric-loss tangent can be explained by the polarization effect. As temperature increases, the electrical conductivity increases due to the thermal activity and mobility of the electrical charge carriers according to the hopping mechanism. Thus, the dielectric polarization increases, increasing the dielectric constant and dielectric loss tangent.

3.4. Temperature dependent magnetic properties

The field dependence of saturation magnetization of as-prepared and sintered samples measured at room temperature is depicted in Fig. 10 for the typical samples ($x = 0.2$ and 0.4). It is observed from Fig. 10 that saturation magnetization increases

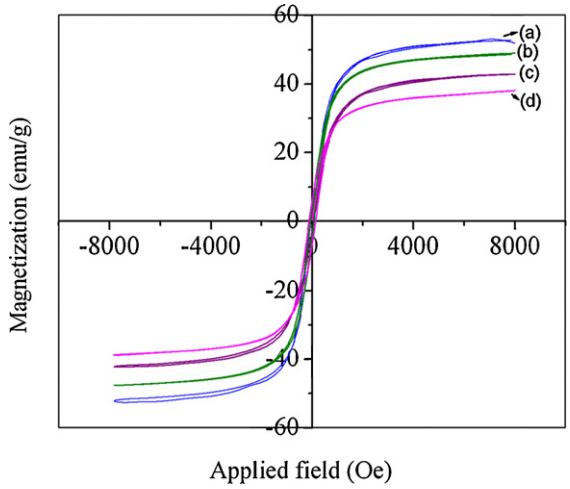

Fig. 10. Variation of magnetization with applied field for sintered (a) $x = 0.2$, (c) $x = 0.4$ and as-prepared (b) $x = 0.2$ and (d) $x = 0.4$ samples.

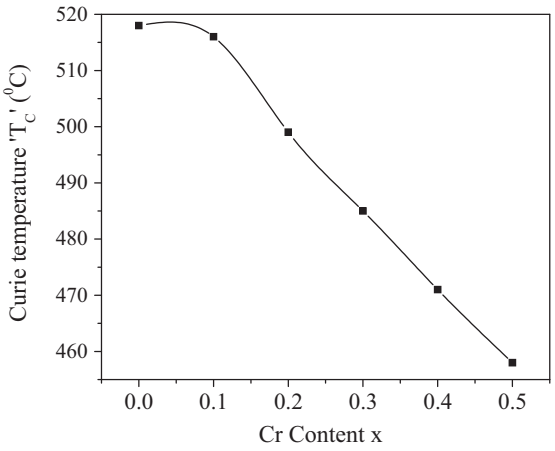

Fig. 12. Variation of Curie temperature with Cr content x.

up to certain applied field above which saturation magnetization remains almost constant. It is observed from Fig. 10 that saturation magnetization decreases with increase in Cr^{3+} content x. The saturation magnetization for the sintered samples is higher as compared to as-prepared samples. The decrease in saturation magnetization for as-prepared samples is related with the effects of the relatively non-reactive surface layer that has low magnetization. This surface effect becomes less significant with increasing particle size and temperature.

Temperature dependent magnetic property such as magnetic susceptibility is carried out in the temperature range of 300 °C up to Curie temperature. The variation of AC susceptibility as a function of temperature and composition x is studied in the present work. Thermal variation of AC susceptibility of all the samples is shown in Fig. 11. The plots of χ_T/χ_{RT} are used to determine the Curie temperature and its variation is shown in Fig. 12. It is clear from Figs. 11 and 12 that the Curie temperature goes on decreasing with the addition of less-magnetic Cr^{3+} content. This is attributed to the decrease in A–B interaction resulting from the replacement of magnetic Fe^{3+} ions by less-magnetic Cr^{3+} ions. According to Neel's model A–B interaction is most dominant in ferrites, therefore, Curie temperature of the ferrites are determined from the overall strength of A–B interaction. The strength of A–B interaction is a function of the number of Fe_A^{+}–O^{2-}–Fe_B^{3+} linkages, which in turn, depends upon the number of Fe^{3+} ions in the formula unit and their distribution amongst tetrahedral (A) and octahedral [B] site. In the present system Fe^{3+} (5 μ_B) ions are replaced by Cr^{3+} (3 μ_B) ions. This results in decreasing the A–B interaction, which lead to decrease in Curie temperature (T_C).

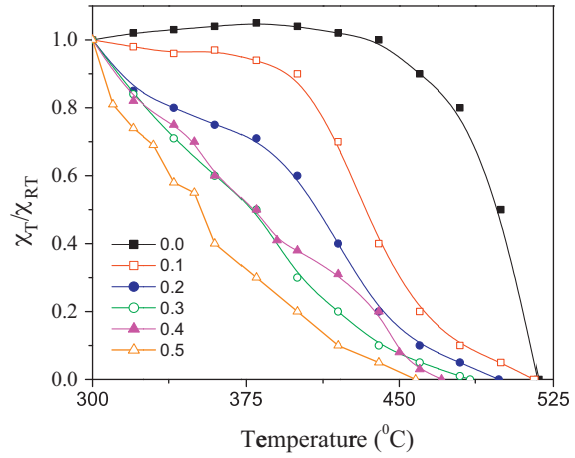

Fig. 11. Plots of χ_T/χ_{RT} versus temperature.

4. Conclusions

The substitution of Cr^{3+} has induced significant changes in the structural, electrical and dielectric properties of Ni–Zn ferrite. The crystallite size is decreases from 37 nm to 21 nm with increasing the Cr^{3+} content x. The Cr^{3+} ions do not participate in the conduction mechanism but limit the degree of $Fe^{2+} \leftrightarrow Fe^{3+}$ transfer, thereby obstructing electron hopping and resulting in an increase in resistivity. Although the resistivity increases with increasing Cr^{3+} content the dielectric constant decreases. The broad peak of the dielectric loss tangent indicates the relaxation time distribution rather than a single relaxation time. Dielectric constant and dielectric loss tangent increases as temperature increases. Saturation magnetization decreases with Cr^{3+} content and showed increased values for sintered samples as compared to as-prepared samples. Curie temperature determined from susceptibility plots shows decreasing trend with increase in Cr^{3+} content.

References

[1] A. Goldman, Modern Ferrite Technology, Van Nostrand Reinhold, New York, 1990.
[2] R.V. Mangalaraja, S. Ananthakumar, P. Manohar, F.D. Gnanam, Initial permeability studies of Ni–Zn ferrites prepared by flash combustion technique, Mater. Sci. Eng. A 355 (2003) 320–324.
[3] U. Enz, in: E.P. Wohlfrath (Ed.), Ferromagnetic Materials, vol. 3, North-Holland, Amsterdam, 1987, p. 1.

[4] R.C. O'Handley, Modern Magnetic Materials – Principles and Applications, Wiley, USA, 2000.
[5] A.M. El-Sayed, Electrical conductivity of nickel–zinc and Cr substituted nickel–zinc ferrites, Mater. Chem. Phys. 82 (2003) 583–587.
[6] C.R. Vestal, Z. John Zhang, Synthesis of $CoCrFeO_4$ nanoparticles using microemulsion methods and size-dependent studies of their magnetic properties, Chem. Mater. 14 (2002) 3817–3822.
[7] A.M. Sankpal, S.S. Suryavanshi, S.V. Kakatkar, G.G. Tengshe, R.S. Patil, N.D. Chaudhari, S.R. Sawant, Magnetization studies on aluminium and chromium substituted Ni–Zn ferrites, J. Magn. Magn. Mater. 186 (1998) 349–356.
[8] S.M. Patange, S.E. Shirsath, S.S. Jadhav, K.S. Lohar, D.R. Mane, K.M. Jadhav, Rietveld refinement and switching properties of Cr^{3+} substituted $NiFe_2O_4$ ferrites, Mater. Lett. 64 (2010) 722–724.
[9] S.E. Shirsath, B.G. Toksha, R.H. Kadam, S.M. Patange, D.R. Mane, G.S. Jangam, Ali Ghasemi, Doping effect of Mn^{2+} on the magnetic behavior in Ni–Zn ferrite nanoparticles prepared by sol–gel auto-combustion, J. Phys. Chem. Sol. 71 (2001) 1669–1675.
[10] D.R. Mane, D.D. Birajdar, S. Patil, S.E. Shirsath, R.H. Kadam, Redistribution of cations and enhancement in magnetic properties of sol–gel synthesized $Cu_{0.7-x}Co_xZn_{0.3}Fe_2O_4$ ($0 \leq x \leq 0.5$), J. Sol–Gel Sci. Technol. 58 (2011) 70–79.
[11] B.D. Cullity, Elements of X-ray Diffraction, Addison-Wesley Publ. Comp. Inc., Reading, Massachusetts, U.S.A., 1956, p. 99.
[12] V.T. Zaspalis, E. Antoniadis, E. Papazoglou, V. Tsakaloudi, L. Nalbandian, C.A. Sikalidis, The effect of Nb_2O_5 dopant on the structural and magnetic properties of MnZn-ferrites, J. Magn. Magn. Mater. 250 (2002) 98–109.
[13] S.M. Patange, S.E. Shirsath, B.G. Toksha, S.S. Jadhav, K.M. Jadhav, Electrical and magnetic properties of Cr^{3+} substituted nanocrystalline nickel ferrite, J. Appl. Phys. 106 (2009) 023914.
[14] J.A. Maxwell, Treatise on Electricity and Magnetism, Clarendon Press, Oxford/London, 1982.
[15] K.W. Wangner, Zur Theorie der Unvollkommenen Dielektrika, Ann. Phys. (Leipzig) 40 (1913) 817–855.
[16] C.G. Koops, On the dispersion of resistivity and dielectric constant of some semiconductors at audiofrequencies, Phys. Rev. 83 (1951) 121–124.
[17] A.K. Jonscher, Dielectric Relaxation in Solids, Dielectric Press, Chelsea, London, 1983.
[18] J. Smit, H.P.J. Wijn, Ferrite, Philips Technical Library, Holland, 1959 , p. 240.
[19] A.K. Singh, T.C. Goel, R.G. Mendiratta, O.P. Thakur, Chandra Prakash, Dielectric properties of Mn-substituted Ni–Zn ferrites, J. Appl. Phys. 91 (2002) 6626.
[20] A.R. Shitre, V.B. Kawade, G.B. Bichile, K.M. Jadhav, X-ray diffraction and dielectric study of $Co_{1-x}Cd_xFe_{2-x}Cr_xO_4$ ferrite system, Mater. Lett. 56 (2002) 188–193.
[21] L.I. Rabkin, Z.I. Novikova, Ferrites, Izd. Nauk. Tekhn., Minsk, 1960p. 146.